Supporting Information

Ligand-Dependent Tuning of Interband and Intersubband Transitions of Colloidal CdSe Nanoplatelets

*Benjamin T. Diroll**

Center for Nanoscale Materials, Argonne National Laboratory 9700 S. Cass Avenue, Lemont, IL, 60439, United States

*bdiroll@anl.gov

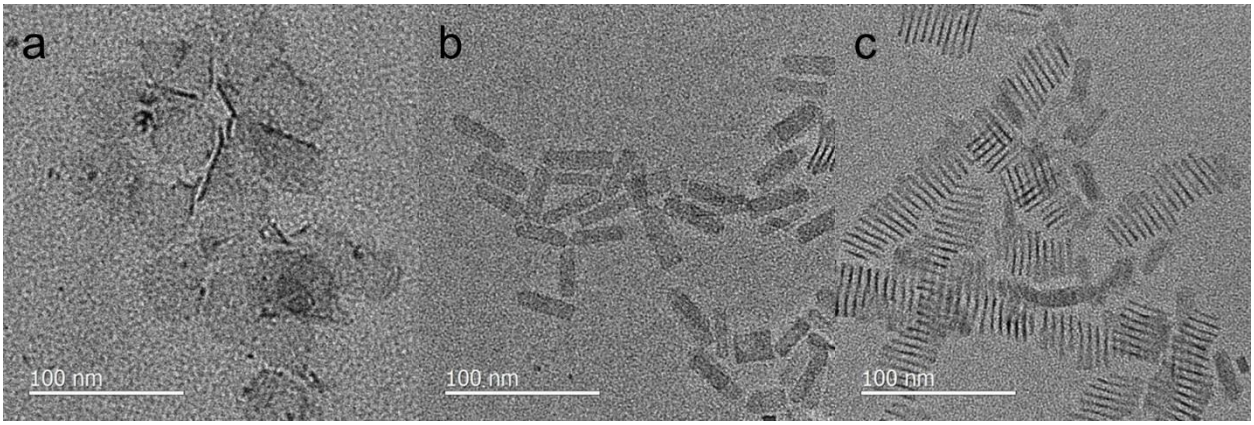

Figure S1. Transmission electron microscopy images of (a) 3.5 ML, (b) 4.5 ML, and (c) 5.5 ML CdSe NPLs.

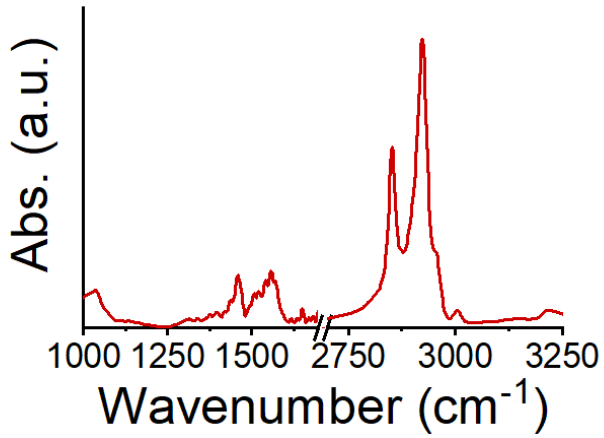

Figure S2. FT-IR absorption spectrum of 5.5 ML NPLs ligand exchanged with bromine-oleylamine ligands.

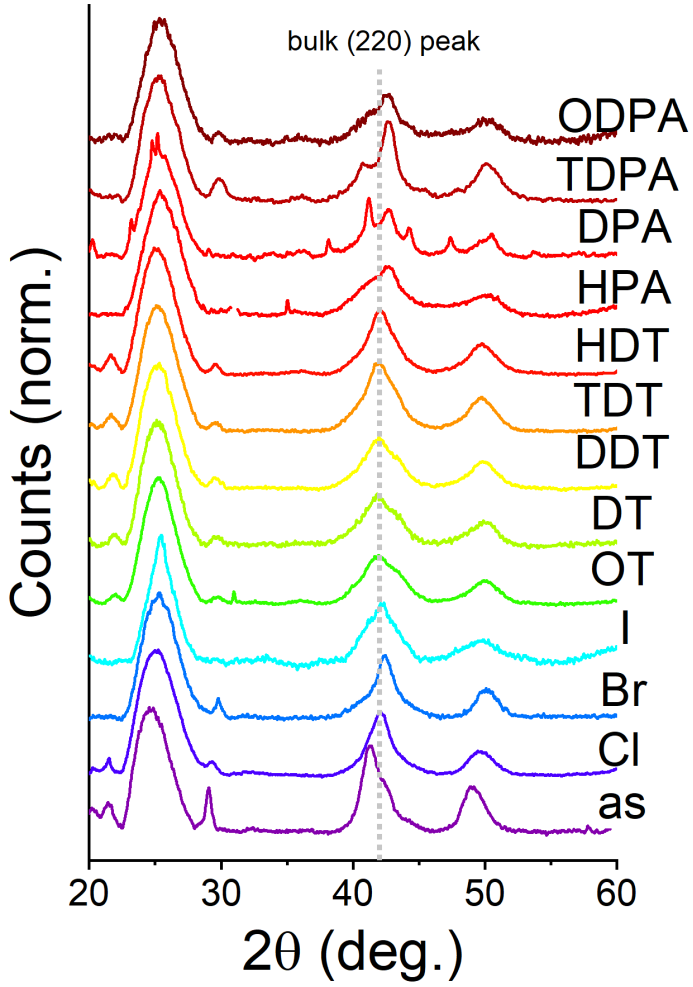

Figure S3. Powder X-ray diffraction data for as-prepared and ligand-exchanged 5.5 ML NPLs used in this work. Many peaks in DPA sample are from residual DPA which was not removed by successive washing with methanol before deposition into a thin film for powder X-ray diffraction.

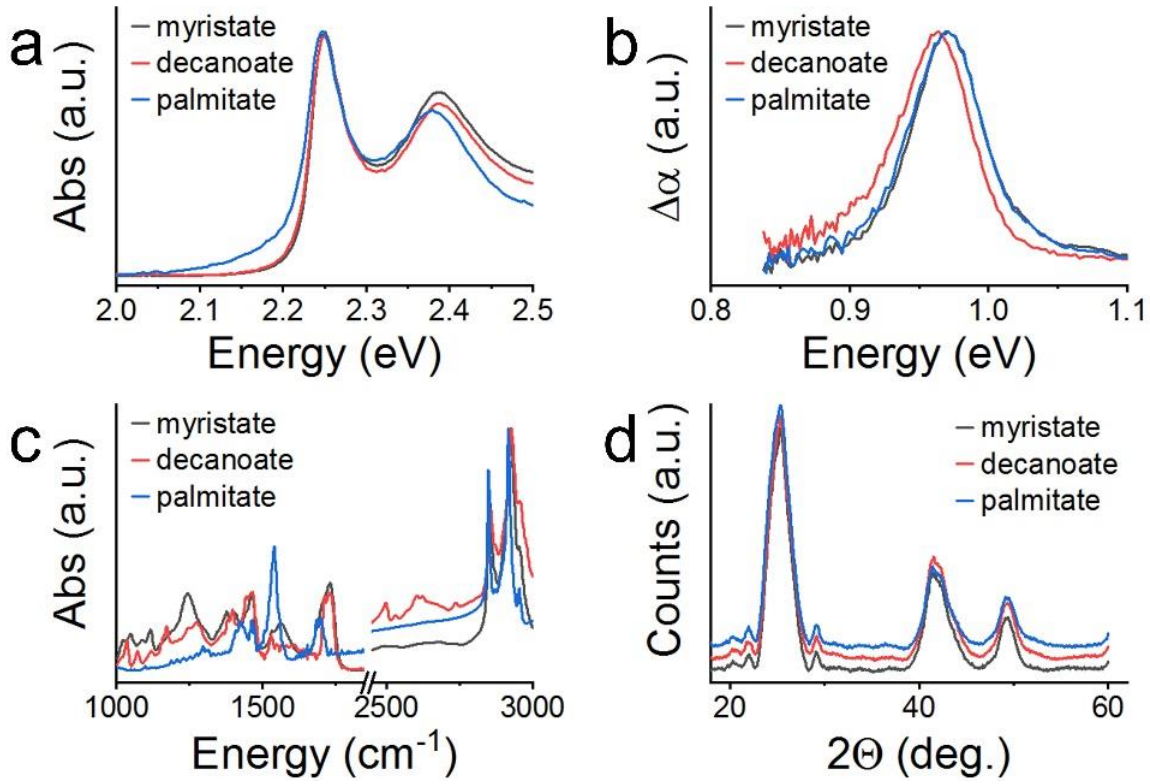

Figure S4. (a) Normalized visible absorption spectra of 5.5 ML NPLs ligand-exchanged with myristic acid, decanoic acid, and palmitic acid. (b) Intersubband absorption spectra collected in the near-IR at 10 ps after 400 nm pump excitation. (c) FT-IR spectra of samples in mid-infrared. (d) Powder X-ray diffraction of exchanged 5.5 ML samples.

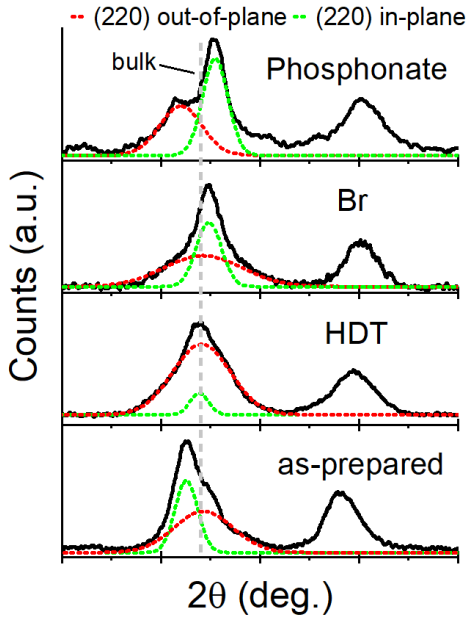

Figure S5. Peak fitting of the (220) family of reflections in a series of as-synthesized and ligand-exchanged 5.5 ML CdSe NPL samples. Powder X-ray diffraction data shown in black were fitted at the (220) peak with a broad reflection (in red) for the thin out-of-plane axis and a narrow reflection (in green) for the larger in-plane axes. Although the in-plane reflection is universally narrower, due to Scherrer broadening, it does not necessarily reflect the full extent of the NPL lattice, as ligand-exchange can also induce greater or less curvature of the NPL.[1]

Table S1. Summary of Powder X-ray diffraction fitting of (220) reflections, including literature.

Exchange Condition	*ab* (220) spacing (Å)	*ab* (220) spacing error (Å)	*c* (220) spacing (Å)	c (220) spacing error (Å)
zb CdSe (bulk)	2.139	-	-	-
as-prepared – 5.5 ML	2.184	0.003	2.141	0.009
chloride – 5.5 ML	2.143	0.005	2.143	0.013
bromide – 5.5 ML	2.128	0.005	2.142	0.017
Iodide – 5.5 ML	2.146	0.004	2.143	0.028
OT – 5.5 ML	2.162	0.019	2.142	0.007
DT – 5.5 ML	2.150	0.018	2.150	0.007
DDT – 5.5 ML	2.156	0.015	2.144	0.008
TDT – 5.5 ML	2.152	0.006	2.146	0.011
HDT – 5.5 ML	2.141	0.008	2.146	0.009
HPA – 5.5 ML	2.112	0.005	2.187	0.029
DPA – 5.5 ML	2.113	0.010	2.176	0.008
TDPA – 5.5 ML	2.115	0.003	2.203	0.009
ODPA – 5.5 ML	2.119	0.025	2.203	0.013
as-prepared-3.5 ML[2]	2.182	-	2.154	-
HDT-3.5 ML[2]	2.134	-	2.163	-
HDPA-3.5 ML[2]	2.119	-	2.167	-

as-prepared-4.5 ML[2]	2.188	-	2.143	-
HDT-4.5 ML[2]	2.145	-	2.148	-
HDPA-4.5 ML[2]	2.127	-	2.160	-
as-prepared-5.5 ML[2]	2.183	-	2.149	-
HDT-5.5 ML[2]	2.155	-	2.150	-
HDPA-5.5 ML[2]	2.129	-	2.161	-
as-prepared-4.5 ML[1]	2.181	-	2.139	-

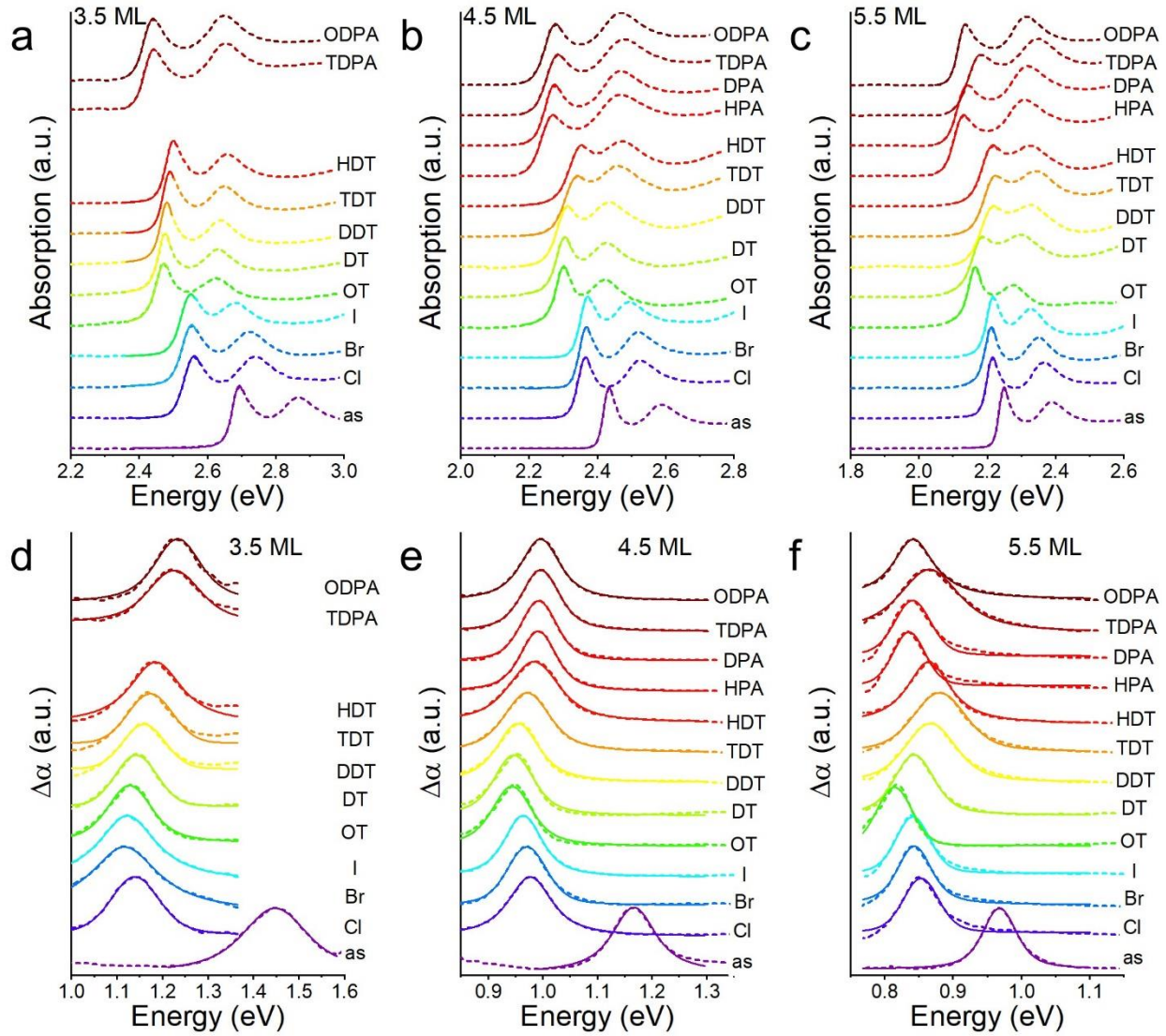

Figure S6. (a-c) Visible absorption spectra of as-prepared and ligand-exchanged solutions of (a) 3.5 ML, (b) 4.5 ML, and (c) 5.5 ML CdSe NPLs. Data are shown in dashed lines. Lorentzian fits of the first excitonic absorption are shown in solid lines. This fitted peak feature is used to define the band-width and energy of the interband transitions. (d-f) Transient absorption spectra collected at 10 ps pump-probe delay in the near infrared using a 400 nm pump excitation for as-prepared and ligand-exchanged solutions of (d) 3.5 ML, (e) 4.5 ML, and (f) 5.5 ML CdSe NPLs. Data are

shown in dashed lines with Voight fits shown in solid lines. Fit data were used to define the energy and band-width of intersubband transitions for the samples.

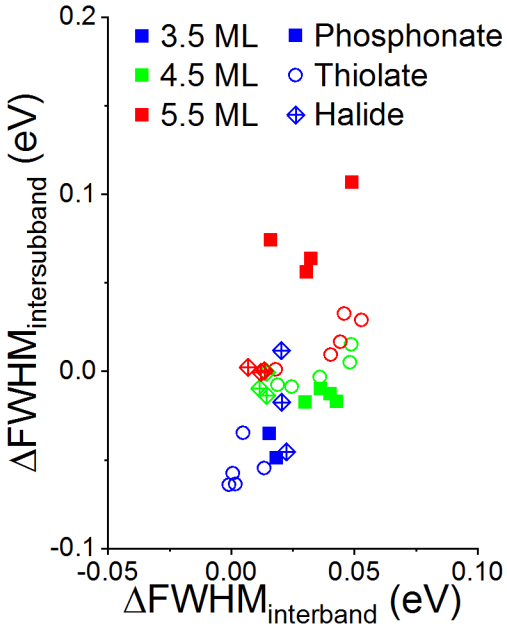

Figure S7. Scatterplot of the changes in FWHM of the interband transition under various ligand-exchange conditions, compared to as-synthesized samples, determined from fitting the low-energy side of first excitonic absorption of the NPLs, versus the change in intersubband FWHM, determined by fitting the peak in the infrared transient absorption spectra.

Effective mass approximation (EMA) modelling. The EMA used in this work was taken without alteration from a previous publication.[3] In short, to estimate the positions of the hole and electron energy levels in CdSe NPLs, the approach described by Efros et al.[4] was followed with updated values used to reflect current understanding of the thickness of NPLs. The position of the bulk bands is calculated within the formalism of the eight-band Pidgeon-Brown model using bulk materials parameters summarized in Table S2.

Table S2. Constant values used in EMA model.

Constant	Value
a	0.608
E_g (eV)	1.66
E_p (eV)	16.5
Δ (eV)	0.39
α	-1.54
γ_1	-0.18
γ_2	-0.65

The energy of the quantum sized levels is found by scaling the band energy by the energy relationship in quantum wells:

$$E_k(n) = \frac{\hbar^2 \pi^2 n^2}{2mL_z^2}$$

where m is the free electron mass and L_z is the thickness of the well and n is the principal quantum number of the envelope wave function. By solving the coupled equations of the Pidgeon-Brown Hamiltonian with the boundary conditions of an infinite potential barrier the positions of the bands are obtained. This results in artificially high confinement energy and a global correction of the effective thickness is used:

$$L_{z,eff} = \frac{wa_0}{2} + 0.32nm.$$

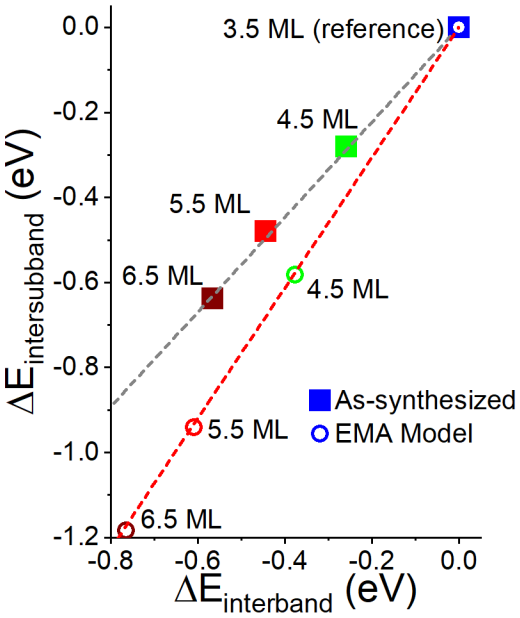

Figure S8. Scatterplot of the changes in interband energy versus those of intersubband absorptions for NPLs of 4.5 ML, 5.5 ML, and 6.5 ML compared to 3.5 ML samples, using (closed squares) experimental data and (open circles) an effective mass model (EMA) data from literature.[3,4] Experimental data for 6.5 ML taken from literature.[3] The dashed gray line is a linear fit to the experimental data points; the dashed red line is a linear fit to the points generated from an EMA model. The linear slope of the points determined from as-synthesized samples is 1.11; the line fitted to those points determined by the EMA model has a slope of 1.58.

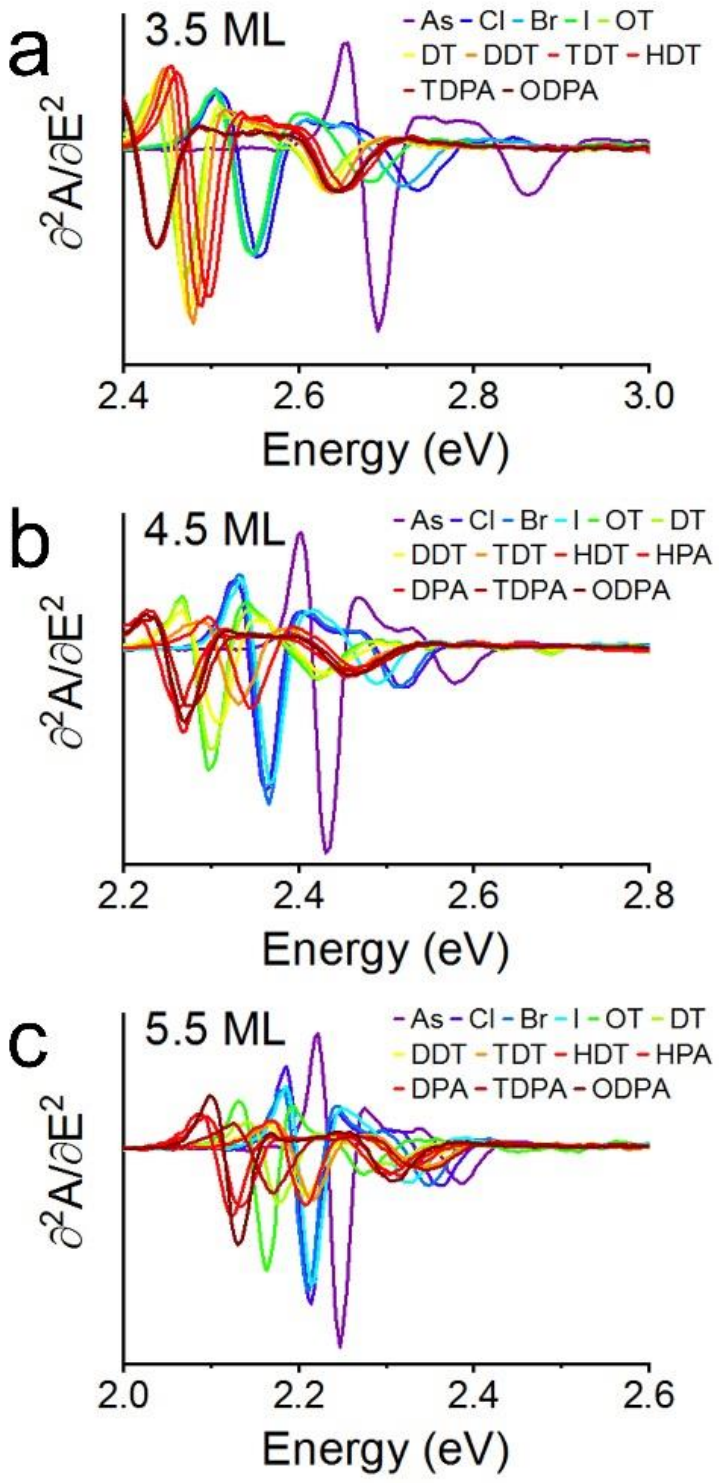

Figure S9. Second derivative of absorption with respect to energy for (a) 3.5 ML, (b) 4.5 ML, and (c) 5.5 ML samples under specified ligand-exchange conditions. Second minima labeled in (a) were used to determine the light-hole (LH) transition energy for analysis of holes states.

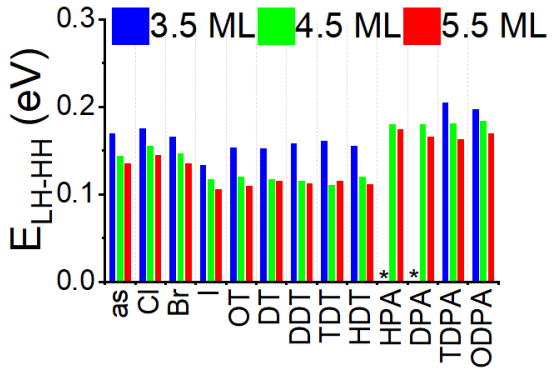

Figure S10. Energy difference of LH and HH states in NPLs as-prepared and with specified ligand exchange conditions. The energy of the HH state is estimated according to fitting of the absorption spectrum in Figure S6; the energy of the LH state is estimated according to second derivative analysis in Figure S9.

References

(1) Dufour, M.; Qu, J.; Greboval, C.; Méthivier, C.; Lhuillier, E.; Ithurria, S. Halide Ligands to Release Strain in Cadmium Chalcogenide Nanoplatelets and Achieve High Brightness. *ACS Nano* **2019**, *13* (5), 5326–5334. https://doi.org/10.1021/acsnano.8b09794.

(2) Antanovich, A.; Achtstein, A. W.; Matsukovich, A.; Prudnikau, A.; Bhaskar, P.; Gurin, V.; Molinari, M.; Artemyev, M. A Strain-Induced Exciton Transition Energy Shift in CdSe Nanoplatelets: The Impact of an Organic Ligand Shell. *Nanoscale* **2017**, *9* (45), 18042–18053. https://doi.org/10.1039/C7NR05065H.

(3) Diroll, B. T.; Chen, M.; Coropceanu, I.; Williams, K. R.; Talapin, D. V; Guyot-Sionnest, P.; Schaller, R. D. Polarized Near-Infrared Intersubband Absorptions in CdSe Colloidal Quantum Wells. *Nat. Commun.* **2019**, *10* (1), 4511. https://doi.org/10.1038/s41467-019-12503-z.

(4) Ithurria, S.; Tessier, M. D.; Mahler, B.; Lobo, R. P. S. M.; Dubertret, B.; Efros, A. L. Colloidal Nanoplatelets with Two-Dimensional Electronic Structure. *Nat. Mater.* **2011**, *10* (12), 936–941. https://doi.org/10.1038/nmat3145.